Pergamon

PII: S0191-8141(97)00068-0

Journal of Structural Geology, Vol. 20, No. 2/3, pp. 211 to 227, 1998

0191-8141/98 $19.00 + 0.00

Shear-zone systems and melts: feedback relations and self-organization in orogenic belts

MICHAEL BROWN and GARY S. SOLAR

Laboratory for Crustal Petrology, Department of Geology, University of Maryland, College Park, MD 20742, U.S.A.

(*Received* 19 *December* 1996; *accepted in revised form* 21 *August* 1997)

Abstract—In orogenic belts, the common spatial and temporal association of granites with crustal-scale shear-zone systems suggests melt transfer from source to upper crust was the result of a feedback relation. In this relation, the presence of melt in the crust profoundly affects the rheology, and induces localization of strain within shear-zone systems. Consequently, melt is moved out of the source preferentially along high-strain zones, which helps the system to accommodate strain. Because actively deforming orogenic belts are non-equilibrium systems, they may generate dissipative structure by self-organization; we interpret crustal-scale shear-zone systems and their associated granites as the manifestation of this self-organization. The architecture and permeability structure are controlled by the type of shear-zone system (transcurrent, normal, reverse or oblique); this is the primary control on melt transfer in orogenic belts. During active deformation, movement of melt is by percolative flow and melt essentially is pumped through the system parallel to the maximum principal finite elongation direction. If a build-up of melt pressure occurs, melt-enhanced embrittlement enables tensile and dilatant shear fracturing, and transfer of melt is by channelized flow.

We illustrate feedback relations between migmatites, crustal-scale shear-zone systems and granites using examples from the Cadomian belt of western France and the northern Appalachian orogen of the eastern U.S.A. In orogenic belts dominated by transcurrent shear, where the maximum principal finite elongation direction may have a shallow to subhorizontal plunge, granite arrested during ascent through the system commonly develops *C–S* fabrics. This suggests percolative flow is not effective in expelling melt from these systems; the resulting build-up of melt pressure enables fracturing and channelized transfer of melt, which crystallizes during persistent deformation (e.g. the St. Malo migmatite belt, Cadomian belt). In contrast, in contractional orogenic belts dominated by oblique-reverse displacement, where the maximum principal finite elongation direction may have a steep to subvertical plunge, granite arrested during ascent through the system generally does not develop *C–S* fabrics. This suggests percolative melt flow during active deformation was effective in avoiding a build-up of melt pressure, probably because buoyancy forces helped melt flow up the maximum principal finite elongation direction. During waning deformation in these systems, however, rates of percolative melt flow decline in response to decreasing strain accommodation, and a build-up of melt pressure results. This enables fracturing and channelized transfer of melt through the shear-zone system; granites are late syntectonic (e.g. the Central Maine belt, northern Appalachian orogen). © 1998 Elsevier Science Ltd.

INTRODUCTION

In active orogenic belts, several important feedback relations are activated between the imposed non-hydrostatic stresses and the thermal evolution. These feedback relations are expressed as interactions between deformation, metamorphism and melting. Thus, local differences in resolved normal stress may determine sites of metamorphic reactions (e.g. Casey, 1980; Ord, 1990; Brodie, 1995), metamorphic reactions may enhance the deformability of a rock (White and Knipe, 1978; Rutter and Brodie, 1995) and localization of strain may motivate recrystallization (e.g. Moecher and Wintsch, 1994). At the grain scale, the distribution of aqueous fluid in crustal rocks may be modified from isolated pores to wetted grain boundaries by deformation (Tullis *et al.*, 1996). This causes a change in the deformation mechanism from intracrystalline plasticity to fluid-assisted grain-boundary diffusive mass transfer plus grain-boundary sliding. In analogous fashion during syntectonic crustal anatexis, the very low permeability threshold at which silicic melt is interconnected in grain-edge channels and along crystal faces (Laporte *et al.*, 1997) also causes a switch in the main deformation mechanism from intracrystalline plasticity to melt-assisted grain-boundary diffusive mass transfer plus grain-boundary sliding (Brown and Rushmer, 1997). In both cases, the switch in deformation mechanisms is accompanied by a significant reduction in crustal strength; this promotes localization of strain and increases bulk transport rates in high-strain zones (Tullis *et al.*, 1996). At the crustal scale, it has been argued that silicic melt may play a role in the initiation and propagation of deformation events in orogenic belts (e.g. Hollister and Crawford, 1986; Hollister, 1993; Brown, 1995), in accommodating strain and localizing deformation (Davidson *et al.*, 1992; Ingram and Hutton, 1994; Tommasi *et al.*, 1994; Nelson *et al.*, 1996), and in aiding the exhumation of high-grade metamorphic core complexes (e.g. Hollister, 1993; Brown and Dallmeyer, 1996).

The mechanism by which crustally derived melt migrates from source to sink in orogenic belts is fundamental to understanding the internal differentiation of the continents, but it is poorly characterized. The common spatial and temporal association of migmatitic metamorphic rocks, crustal-scale shear-zone systems and granites in orogenic belts suggests a relationship, but which is cause and which is consequence has proven

difficult to decide. Evidence that crystallization of melt occurred synchronously with deformation, particularly the widespread occurrence of pervasive ductile shear bands within syntectonic granites in transcurrent shear-zone systems (e.g. Berthé *et al.*, 1979; Gapais, 1989; Gapais and Balé, 1990), allows two alternative explanations: either melt transfer through the crust in orogenic belts is controlled by crustal-scale shear-zone systems and some transferring melt is arrested during ascent to become emplaced in these systems (D'Lemos *et al.*, 1992; Hutton and Reavy, 1992; Brown, 1994; Román-Berdiel *et al.*, 1997; Brown and Solar, in review); or strain localization within crustal-scale shear-zone systems is induced by the presence of bodies of partly crystallized magma that are rheologically weaker than the surrounding crustal rocks (Tommasi *et al.*, 1994; Neves *et al.*, 1996).

These two interpretations may not be mutually exclusive, but may be different views of the same feedback relation. In this feedback relation, nucleation and growth of the shear-zone system occur synchronously with melting and melt migration; presence of melt in the crust profoundly affects its rheology (Rutter and Brodie, 1992), which will localize deformation, while movement of melt out of the source is an important mechanism by which partially molten crust accommodates strain (Brown, 1995). An apparent implication of this feedback relation is that the growth rate of the shear-zone system and the migration rate of the melt should be similar, because it is the presence of melt that is the weakening mechanism (Neves *et al.*, 1996). However, the rate of melt production in relation to the rate of melt flow is also an important control. Heat is consumed as latent heat of melting, so that the rate of melt production depends on the thermal evolution of the system. For the case of crustally derived granite melt, this suggests that the feedback relation will be most effective during the late prograde and peak-T parts of the P–T evolution in thickened orogenic belts. We argue below that the effectiveness of percolative melt flow is a function of the type of shear-zone system (transcurrent, normal, reverse or oblique) and the rate of deformation. If the rate of melt production exceeds the rate at which it can be expelled by percolative flow, then build-up of melt pressure leads to melt-enhanced embrittlement (Davidson *et al.*, 1994) and channelized transfer of melt batches along tensile fractures and dilatant shear fractures/high-strain zones.

Feedback relations and self-organization

Feedback relations between deformation and melting during orogenesis are activated under non-equilibrium conditions. The introduction of fluctuations into a system far from equilibrium (e.g. due to melting) leads to instabilities, and new types of structure and function develop in response (e.g. localization of deformation into high-strain zones and migration of melt through these zones). The feedback causes amplification of appropriate fluctuations; if the pattern associated with a fluctuation appears stable after attaining a macroscopic amplitude, it is termed a dissipative structure (Ortoleva, 1994). Such evolution is a self-determining sequence of mutual feedback relations among fluctuations, structure and function; it leads to increasing complexity and order within the system (Nicolis and Prigogine, 1977). Dissipative structures provide a good example of disequilibrium as a source of order. If fluctuations can be introduced, then no system driven far from equilibrium is stable structurally, and any system may spontaneously generate dissipative structure by self-organization (Nicolis and Prigogine, 1977; Ortoleva, 1994). Actively deforming orogenic belts are examples of non-equilibrium systems that may generate dissipative structure by self-organization, and we interpret crustal-scale shear-zone systems and their associated granites as the expression of this self-organization.

Melting under applied stress

Exhaustive experimental studies under applied hydrostatic stress conditions have shown that silicic melt will form an interconnected network in common crustal protoliths (e.g. Holness, 1997; Laporte *et al.*, 1997; and references therein). Additionally, rock-forming minerals show some degree of anisotropy of surface energies, particularly ferromagnesian phases that are likely to dominate the melt geometry in partially molten crust. Anisotropy leads to the development of planar, rational, low-energy crystal faces in contact with the fluid. Thus, melt geometries during anatexis are likely to be controlled by anisotropic hornblende and biotite rather than quartz and feldspar (Wolf and Wyllie, 1991; Laporte and Watson, 1995), and the interconnected network that results will comprise grain-edge tubes and planar pores along crystal faces (Brown and Rushmer, 1997). Although the permeability threshold of partially molten crustal rocks is likely to be very low (a reasonable upper limit of 3.4 vol.% has been suggested by Laporte *et al.* (1997)), the viscosity of typical crustal melts makes segregation inefficient at low melt fractions and melt is nearly stagnant at percentages below 5–10 vol.% in the crust (Brown *et al.*, 1995; Laporte *et al.*, 1997). Melt segregation is unlikely to be driven by buoyancy forces alone (Brown *et al.*, 1995; Rutter and Neumann, 1995; Rutter, 1997); instead, melt concentrates at sites decided by the local pressure gradients that occur in a source subject to an imposed non-hydrostatic stress field (Brown and Rushmer, 1997).

As the equilibrium for a melt-producing reaction is overstepped, sites of initial melting may be selected based on factors beyond the presence of the appropriate phase assemblage. The Earth's crust is anisotropic and in a state of non-hydrostatic stress, so that differential stress will vary within any particular volume. Close to the equilibrium P–T condition for a metamorphic reaction, small heterogeneities in resolved normal stress may help in

overstepping the reaction stability. Once a reaction starts, the rock at that site will weaken (White and Knipe, 1978). For reaction sites with an elongate shape, such as those expected at low vol.% melting, the orientation of the long axis with respect to the maximum principal compressive stress determines whether reaction weakening will result in an increase or decrease in stress (Casey, 1980). As a result, a particular reaction may be inhibited or promoted. Shear instabilities may develop at sites where the reaction is promoted. In this way, melting may begin at sites of higher resolved normal stress for solidi with negative dP/dT (high a_{H_2O} volatile phase-present melting) and at sites of lower resolved normal stress for solidi with positive dP/dT (low a_{H_2O} volatile phase-absent melting). For example, melting at high a_{H_2O} causes a reduction in strength at the sites of initial melting. This results in an increase in stress on melt pockets oriented at an angle $>45°$ to the maximum principal compressive stress, and melting is promoted at these sites. Thus, shear instabilities may develop at these sites after some critical volume of melt is achieved. These selective sites of strain accommodation grow by a feedback relation to form migmatite leucosomes; melt is concentrated in leucosomes driven by the difference in normal stresses, which enhances their ability to accommodate strain. The feedback relation between deformation and melting creates a dynamic rheological environment.

Transpressional orogens

The self-organization phenomena of interest in this paper involve localization of strain due to melting and the redistribution of mass by melt migration to accommodate strain. To investigate these phenomena we consider feedback relations between high a_{H_2O} volatile phase-present melting and synanatectic deformation in two transpressional orogens, the Neoproterozoic Cadomian belt of western France and the Lower Paleozoic Appalachian orogen of eastern North America. In many transpressional orogenic systems, regional metamorphism is likely to be driven by thermal relaxation of thickened sedimentary basins, aided by horizons of unusually high heat production or by enhanced subcrustal heat flux (e.g. Chamberlain and Sonder, 1990; Royden, 1993; Thompson *et al.*, in press). Deformation in transpressional orogens involves both coaxial and non-coaxial components of strain. In the St. Malo migmatite belt, part of the Cadomian belt, the coaxial component of strain was accommodated in part by melt migration through the belt, while the non-coaxial component of strain was important in enabling magma transfer through the crust in transcurrent shear-zone systems marginal to the belt (Brown, 1995). In contrast, in the Central Maine belt, part of the northern Appalachian orogen, oblique contractional shear was dominant during dextral transpression (Solar, 1996), and regional-scale strain partitioning exerted an important control on melt flow pathways and sites of pluton emplacement (Brown and Solar, in review).

MIGMATITES AND GRANITES IN THE CADOMIAN BELT, WESTERN FRANCE

Structure of the Cadomian belt

The evolution of the Cadomian belt has been interpreted as the consolidation of calc-alkaline continental arc and intra-arc basin complexes with behind-arc marginal-basin to within-plate basin sequences at an obliquely convergent plate-boundary zone along the northern margin of a Gondwana supercontinent (e.g. Cogné and Wright, 1980; Graviou and Auvray, 1985; Graviou *et al.*, 1988; Strachan *et al.*, 1989; Brown *et al.*, 1990; Brown, 1995). In this model (Fig. 1a), the North Armorican shear-zone system (NASZ) separates elements of the North Armorican composite terrane (NACT), composed of Neoproterozoic volcanic and sedimentary basins structurally inverted and deformed during the Cadomian orogeny, from the Central Armorican terrane (CAT), in which the main deformation and regional metamorphism of the Neoproterozoic sedimentary sequences occurred during the Variscan orogeny. The NACT represents a S-verging strike-slip wedge that soles at mid-crustal levels above a highly reflective lower crust (Brun *et al.*, 1997).

The NACT comprises four terrane elements separated by steeply dipping shear zones and faults (Fig. 1). From north to south these are the arc-related Trégor–La Hague (TLHT) and St. Brieuc (SBT) terranes, which are separated by the Fresnaye shear-zone system (FSZ) from the behind-arc marginal-basin to within-plate basin sequences of the St. Malo (SMT) and Mancellian (MT) terranes. The FSZ records sinistral transcurrent displacement (Brun and Balé, 1990; Treloar and Strachan, 1990); it represents a fundamental crustal structure, as reflected in the contrast in both surface geology and geophysical signatures across this zone (Brun and Balé, 1990). Southward-younging of major tectonothermal events in the NACT was interpreted by Brown (1995) to reflect regionally diachronous and hinterland-propagating orogenic deformation across an obliquely convergent plate-boundary zone, consequent upon some singularity at the trench. Additionally, the inferred age of accumulation of the Neoproterozoic sedimentary sequences is southward-younging in the constituent terranes of the NACT, and across the NASZ to the CAT (Brown, 1995).

The St. Malo (SMT) and Mancellian (MT) terranes

The SMT and MT are separated by the transcurrent Cancale shear-zone system (CSZ; Fig. 1), within which the high-strain zone at Port Briac (Fig. 2a) records sinistral transcurrent displacement (Brun and Balé, 1990; Treloar and Strachan, 1990). The migmatites and

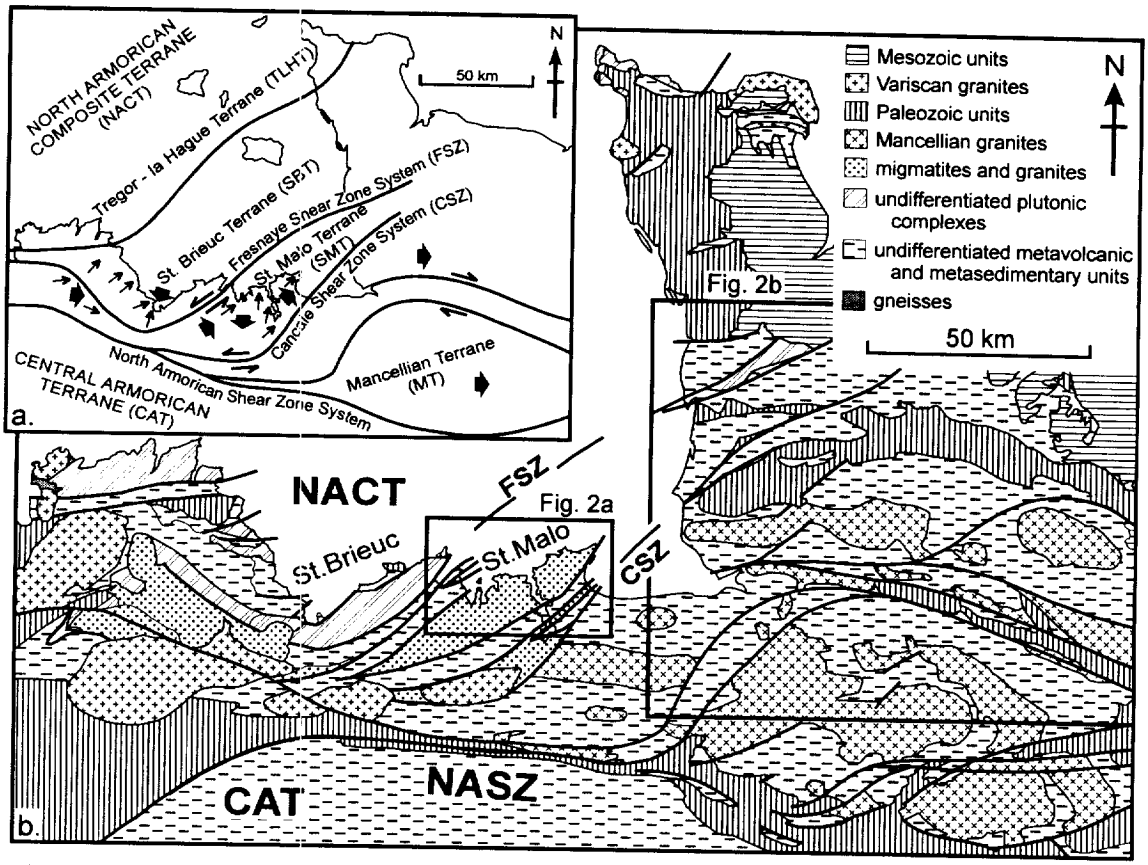

Fig. 1. (a) Simplified terrane map of the Cadomian belt, western France. Thin arrows represent generalized orientations of the dominant mineral elongation lineation, half-arrows represent sense of shear along transcurrent zones and broad arrows represent generalized sense of tectonic transport. (b) Simplified geological map of the Cadomian belt to show the major tectonostratigraphic units. The North Armorican composite terrane (NACT) is separated from the Central Armorican terrane (CAT) by the North Armorican shear-zone system (NASZ). The St. Malo terrane is bounded to the northwest by shear zones of the Fresnaye shear-zone system, including the Fresnaye shear zone (FSZ), and to the southeast by shear zones of the Cancale shear-zone system, including the Cancale shear zone (CSZ). The two rectangles indicate the areas covered by Fig. 2(a & b), respectively.

the granites within these two terranes are coeval at *ca* 540 Ma (Pasteels and Doré, 1982; Peucat, 1986; Dallmeyer *et al.*, 1993), and have similar geochemical features (Brown and D'Lemos, 1991) and Nd isotopic signatures (D'Lemos and Brown, 1993). The SMT and MT are likely to represent different structural levels of a once continuous tectonic unit (Brown and D'Lemos, 1991) inboard of the Cadomian arc.

Post-metamorphic cooling at *ca* 570–565 Ma in the SBT was interpreted by Brown (1995) to record uplift and exhumation due to progressive accretion of the TLHT–SBT composite terrane with the behind-arc marginal-basin and within-plate units, now represented by the SMT–MT composite terrane. These sedimentary basins represented rheologically weaker domains in comparison with the outboard TLHT–SBT composite terrane, which acted more like a rigid indenter (cf. Peltzer *et al.*, 1982; Tommasi *et al.*, 1995). Basin inversion by sinistral transpression led to progressive deformation of the Neoproterozoic sedimentary sequences in the SMT, synchronous with prograde metamorphism and anatexis (Brown, 1995). The low-strength SMT accommodated both contractional and transcurrent components of the transpressional deformation. This resulted in highly heterogeneous strain fields in which the rheological heterogeneities induced localization of strain within shear-zone systems both within and marginal to the belt (Fig. 2a). In contrast, the MT accommodated transpressional deformation by development of a sinuous system of narrow transcurrent high-strain zones that allowed eastward extrusion of the terrane (Fig. 1). The geometric relationship between the narrow high-strain zones and cleavage in the intervening blocks varies across the terrane (Fig. 2b). On the northern margin, counter-clockwise-transecting cleavage is consistent with sinistral transpression. However, clockwise-transecting cleavage internal to the terrane suggests dextral transpression. We interpret this to reflect displacement of individual blocks at different rates during overall eastward extrusion of the MT.

Within the SMT, metamorphism in the St. Malo migmatite belt is of a high T–low P type, in which the stability of muscovite + quartz has been exceeded, biotite + sillimanite was generally stable, and garnet and cordierite occur only rarely (Brown, 1995). P–T conditions were middle crustal, and anatexis is likely to have

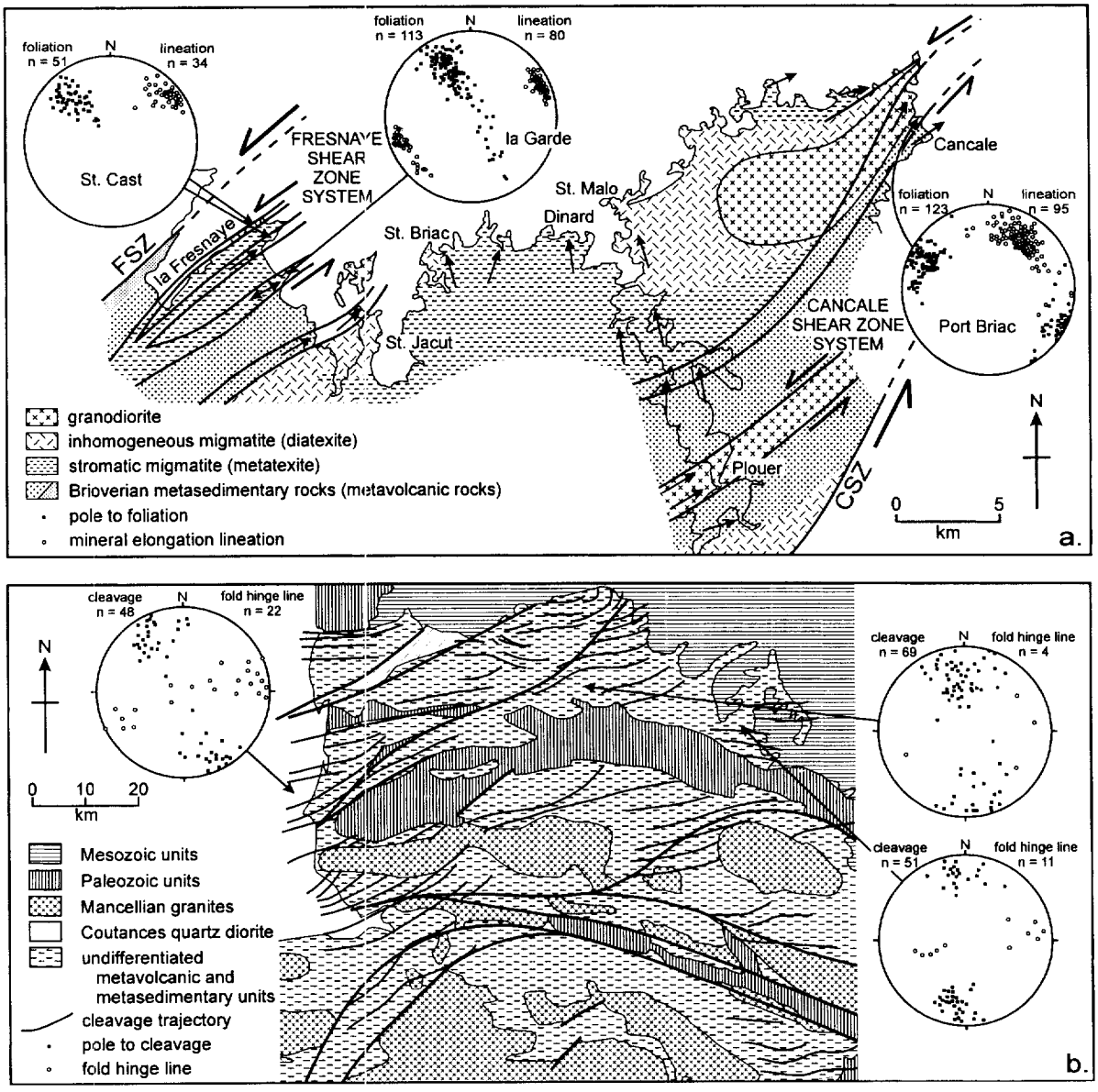

Fig. 2. (a) Simplified geological map of part of the St. Malo terrane (based on data from Brown, 1974,1978,1979, 1995; Brun and Balé, 1990; Treloar and Strachan, 1990; D'Lemos *et al.*, 1992). Arrows represent generalized orientations of the dominant mineral elongation lineations, and half-arrows represent the sense of shear along transcurrent zones. Stereograms are lower-hemisphere (Schmidt) projections of poles to foliation (black squares) and mineral elongation lineations (open circles) from transcurrent high-strain zones. (b) Simplified geological map of part of the Mancellian terrane, particularly to show the relations between inferred high-strain zones, cleavage trajectories and granite plutons (based on data from Dupret *et al.*, 1990; Brown, 1995). Stereograms are lower-hemisphere (Schmidt) projections of poles to cleavage (black squares) and fold hinge lines (open circles) from blocks between narrow transcurrent high-strain zones in the northern part of the terrane.

occurred under water-rich volatile phase-present (high a_{H_2O}) conditions (Brown, 1979, 1995). For the Mancellian granites, *P–T* conditions of magma generation were probably middle to lower crustal, as suggested by garnet with inclusion trails of sillimanite that occur in the Athis granite in particular (Brown, 1995). The Mancellian granites were emplaced into the upper crust.

Within the St. Malo migmatite belt, early structures record contractional thickening during a progressive deformation in which bedding-parallel foliation in high-grade metasedimentary rocks and stromatic layering in migmatites formed and were folded due to perturbations in the flow regime (Fig. 3a) (Brown, 1978, 1995). At the outcrop scale, localization of strain and formation of dilatant high-strain zones in stromatic migmatites suggest coaxial strain was limited by the rate at which melt was expelled by percolative flow. As a result, the increased non-coaxial strain was accommodated by development of dilatant shear-zone systems that enabled more effective melt expulsion. High-strain zones within this system are present at all scales, from the individual outcrop (Fig. 3a & b) to the map scale. They are shallow N-dipping top-to-the-south (N-plunging mineral elongation lineation; Fig. 2a) and anastomose around elongate

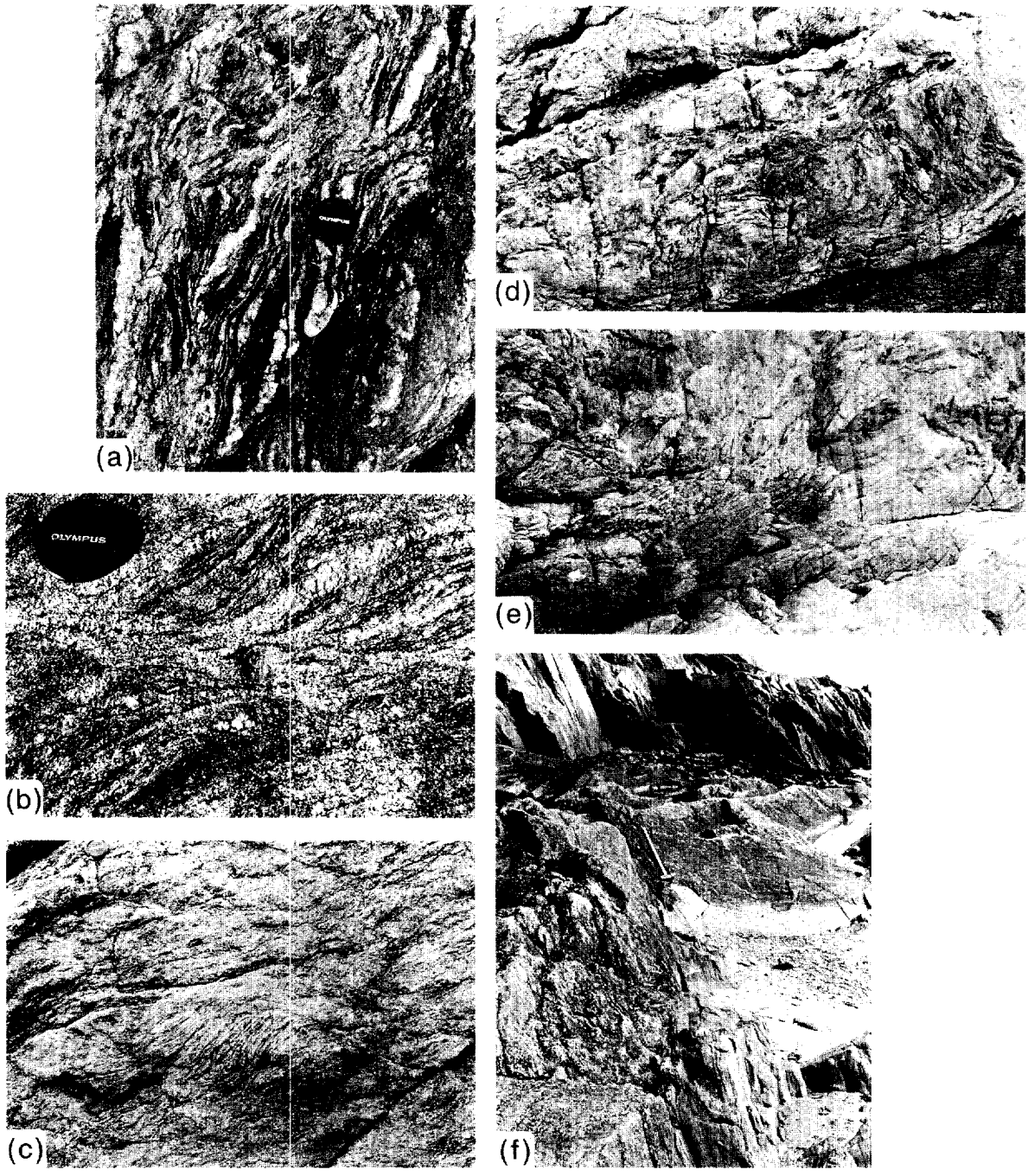

Fig. 3. Examples of relations from the St. Malo migmatite belt, France. (a) Small mesoscopic N-dipping top-to-the-south granite-filled high-strain zone within stromatic migmatite (metatexite), St. Jacut. (b) Leucosome-filled anastomosing high-strain zones within high-grade stromatic migmatite (metatexite), St. Briac. (c) Foliated inhomogeneous migmatite (schlieric diatexite) within which occurs a lower strain zone block of stromatic migmatite bounded by sheared margins, view to the east-northeast, Dinard. (d) Meter-scale shallow N-dipping (to left) top-to-the-south high-strain zone (upper and lower parts of field of view along which anatectic granite has been emplaced), St. Jacut. (e) Decameter-scale shallow N-dipping (to left) top-to-the-south high-strain zone (lower half of photograph) into which was emplaced flow-foliated anatectic granite with occasional schlieren and small enclaves of stromatic migmatite, St. Jacut. (f) Steep foliation and shallow ENE-plunging mineral elongation lineation at the contact between Cancale granodiorite (to the north, left) and mylonitic Brioverian metasediments with cordierite porphyroblasts (to the south, right), Port Briac.

ENE-trending pods of anatectic granite (Fig. 3d). The anatectic granite exhibits flow foliation (Fig. 3e). The high-strain zones were melt-bearing as evidenced by the granite preserved in them (Fig. 3b & d). This is an example of a feedback relation during active deformation of partially molten crustal rocks in which the evolution to dissipative structure by self-organization enabled more effective flow of melt to accommodate the coaxial strain. Melt movement through the migmatites took place along the shallowly N-dipping top-to-the-south high-strain

zones, along the anisotropy of permeability parallel to the maximum principal finite elongation direction (expressed by the mineral elongation lineation), up-plunge in the direction of hanging-wall transport.

Marginal to the St. Malo migmatite belt, anatectic granite (Fig. 3f) is found in ENE-striking subvertical sinistral-transcurrent high-strain zones within crustal-scale shear-zone systems (shallowly ENE-plunging mineral elongation lineation; Fig. 2a), in the wall rocks of which cordierite exhibits complex microstructural relations with the mylonitic foliation consistent with pulsed melt transfer during active deformation (D'Lemos *et al.*, 1992). Overall, the contractional domain enclosed by the transcurrent shear-zone systems (between the FSZ in the west and the CSZ in the east; Fig. 2a) represents a lower strain domain. The shallow-dipping reverse high-strain zones within, and the steeply-dipping transcurrent high-strain zones marginal to, the St. Malo migmatite belt essentially were coeval, reflecting strain partitioning during progressive deformation. The granites exhibit *C–S* fabrics that record pervasive ductile strain accumulated during crystallization and subsolidus cooling (Gapais and Balé, 1990; Treloar and Strachan, 1990; D'Lemos *et al.*, 1992); this suggests emplacement during ascent through the crust and localization of deformation within the granites as they crystallized.

Summary

Thickening of the Neoproterozoic sedimentary basins from *ca* 570 Ma was a consequence of contraction driven by indentation during progressive sinistral accretion of rigid outboard arc-related terranes with rheologically weaker sedimentary basins inboard. As the SMT basin started to invert, the MT basin was still extending and receiving sediment. High-*T* metamorphism was likely to be a consequence of thermal relaxation of the moderately overthickened sedimentary basin (Brown, 1995). Within *ca* 30 Ma, anatexis had further weakened the crust, particularly within the SMT, and sinistral transpression extended across the behind-arc region which drove eastward extrusion of the MT. Feedback relations between the far-field tectonic stresses and crustal anatexis controlled deformation of the belt. The sinuous nature of the transcurrent shear-zone systems (Fig. 1) would have impeded easy strike-parallel motion and would have limited lateral displacements of the wall rocks. Continued deformation was made possible by volume loss due to movement of melt out of the SMT. *C–S* fabrics within granites in transcurrent high-strain zones imply crystallization during active deformation. Ascent of the Mancellian granite melts is inferred to have been channelized in fractures within narrow high-strain zone branches of the steeply oriented transcurrent shear-zone system to the east; granite plutons were constructed by lateral fracture propagation into lower strain domains between these branches (Brown and D'Lemos, 1991; Brown, 1995) as the melt approached the brittle–plastic transition within the crust (cf. Brown and Solar, in review). Thus, the Mancellian granites are interpreted to represent ponding at shallower levels of granitic melt similar to that frozen during transfer in the sinistral-transcurrent shear-zone systems marginal to the St. Malo migmatite belt.

MIGMATITES AND GRANITES OF THE CENTRAL MAINE BELT, NORTHERN APPALACHIAN OROGEN, U.S.A.

Structure of the northern Appalachians

In the northern Appalachians, Paleozoic rocks in New England have been divided into several tectonostratigraphic provinces (Fig. 4). Two of these, the Bronson Hill belt (BHB) and the Central Maine belt (CMB), contain structures believed to have formed during the Devonian (Eusden and Barreiro, 1988; Smith and Barreiro, 1990; Getty and Gromet, 1992; Peterson and Robinson, 1993). The BHB contains a series of structural culminations or

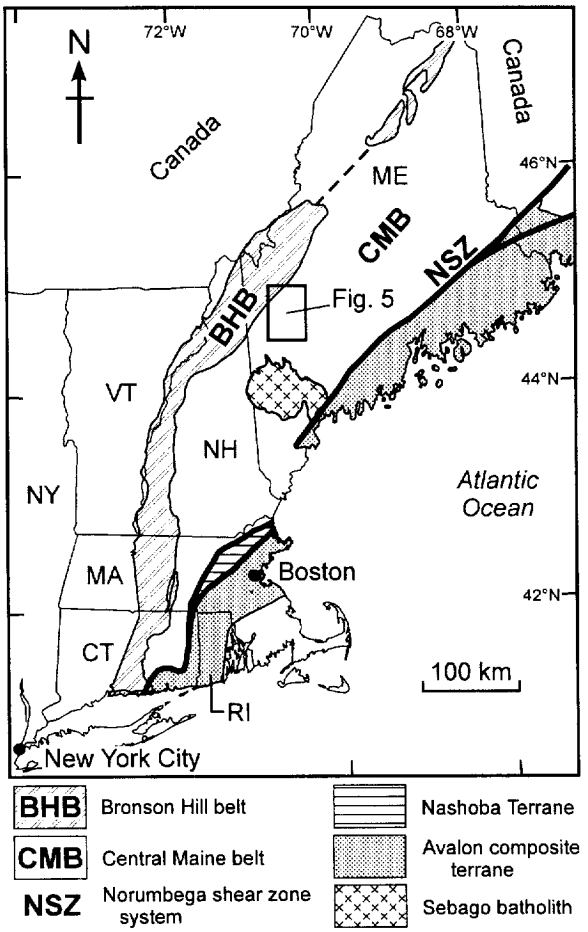

Fig. 4. Map of New England (U.S.A.) to show the location of the Central Maine belt (CMB) in relation to the Bronson Hill belt (BHB) to the northwest, and the Norumbega shear-zone system (NSZ) and the Avalon composite terrane to the southeast. The rectangle to the north of the Sebago batholith indicates the area covered by the map in Fig. 5(a & b). ME, Maine; NY, New York; VT, Vermont; NH, New Hampshire; MA, Massachusetts; CT, Connecticut; and RI, Rhode Island.

domes, with cores of Neoproterozoic and late Ordovician basement. The CMB to the east is composed of highly deformed and metamorphosed late Ordovician and Silurian continental slope-rise sediments overridden by early Devonian flysch (Hatch *et al.*, 1983). In New England, dextral transpressive deformation that began during the Silurian–Devonian was partitioned into synchronous oblique and transcurrent shear-zone systems during the Devonian–Carboniferous. Consequently, in Maine, displacement changes across strike from dextral-transcurrent in the Norumbega shear-zone system (NSZ; Fig. 4) to oblique dextral-reverse in the CMB. The grade of metamorphism within the CMB varies from greenschist facies to upper amphibolite-granulite facies (Chamberlain and Robinson, 1989). The metamorphism is of high T–low P type and includes the extensive development of migmatites along the 'central Acadian metamorphic high' from central Massachusetts and southern New Hampshire (Schumacher *et al.*, 1990; Lathrop *et al.*, 1994; Allen, 1996) into central Maine (Guidotti, 1989; DeYoreo *et al.*, 1989; Solar, 1996).

West-central Maine

A foliation form line map (Fig. 5a), based on detailed mapping by Solar (1996) in the Tumbledown Mountain area (Fig. 6) and extensive field checks of published maps (Moench, 1971; Moench and Hildreth, 1976; Pankiwskyj, 1978), shows that deformation was inhomogeneous. All of the metasedimentary rocks represented on the map exhibit high strain, but the strain has been partitioned into anastomosing zones of higher strain that surround lenses of lower strain. The zones of higher strain developed in stratigraphic units with a higher proportion of metapelite, which are rheologically weaker as a result (Fig. 5b). Thus, the first-order partitioning of strain was controlled by the bulk rheology of stratigraphic units, determined by the relative proportion of metapsammite to metapelite. These pre-existing rheological heterogeneities determine sites of strain localization; they are important in the middle and lower crust, and at higher grades of metamorphism, because the material properties of crustal rocks in these circumstances favor a more homogeneous distribution of strain.

Below the solidus, higher strain zones are characterized by pervasive parallelism of both planar and linear structures, including transposed bedding, tight to isoclinal folds of compositional layering and metamorphic fabrics. The foliation is steeply SE-dipping with moderate NE-plunging lineation (Figs 6 & 7a); overall, this fabric is a flattening type with $S > L$. A scale-repeating geometry of inhomogeneous strain is typical of higher strain zones, which contain internal smaller-scale anastomosing zones of higher strain that wrap around attenuated lens-shaped areas of lower strain.

Zones of lower strain are characterized by non-parallelism of planar and linear structural elements (Fig. 6). Folds defined by compositional layering are open to closed, with variably developed axial-planar metamorphic fabrics. Within zones of lower strain, foliation is weak or absent, and the fabric is of constrictional type with $L > S$. Traverses across zones of lower strain toward their boundaries with higher strain zones show progressive rotation of lineation, foliation and compositional layering into parallelism with these structures inside neighboring higher strain zones.

Within higher strain zones, microstructures in thin sections cut parallel to mineral elongation lineation and perpendicular to foliation (Fig. 8a), and perpendicular to mineral elongation lineation (Fig. 8b), illustrate synkinematic growth of garnet and staurolite porphyroblasts in pelitic schist, and confirm the $S > L$ fabric. Asymmetric quartz-rich pressure shadows around garnet and biotite 'fish' show reverse-dextral (i.e. southeast side up-to-the-southwest) displacement. By comparison, microstructures in zones of lower strain, as viewed in thin sections cut parallel to mineral elongation lineation and perpendicular to the weak foliation (Fig. 8c), and perpendicular to mineral elongation lineation (Fig. 8d), show a poorly developed planar microstructure defined by muscovite with the lineation defined by synkinematic porphyroblasts of biotite and staurolite. This suggests dominantly constrictional strain in these zones synchronous with metamorphism.

A consequence of the southeast side up-to-the-southwest relative displacement was juxtaposition of anatectic migmatites of the Tumbledown Anatectic Domain (TAD) in the southeast with non-anatectic rocks to the northwest (Figs 5 & 6). The contact between anatectic and non-anatectic domains occurs mostly within higher strain zones but crosses zone boundaries (Figs 5 & 6). This does not imply that the contact between the two domains cross-cuts structures. Instead, mapping shows the contact is tightly folded with limbs essentially parallel to foliation. The asymmetric folding of this contact suggests continuation of ductile deformation within the higher strain zones following juxtaposition of the TAD with the surrounding non-anatectic rocks.

Above the solidus, higher strain zones exhibit similar features to those below the solidus, but increased biotite in the mode and the occurrence of sillimanite suggest residual chemistry due to melt loss (Fig. 7b). In contrast, zones of lower strain are characterized by inhomogeneous migmatites with $S > L$ fabrics (Fig. 7f), which implies loss of melt from these zones as well. Overall, these inhomogeneous migmatites exhibit lower strain than recorded by stromatic migmatites in higher strain zones, and lower strain than recorded by zones of lower strain below the solidus. This suggests that anatexis has wiped out the early strain history and reset the strain gauge.

Leucogranite occurs as boudinaged sheets in higher strain zones of the non-anatectic domain; where asymmetric, they show a dextral component of displacement. Therefore, the leucogranites represent migrating magma arrested during ascent before orogenic deformation had

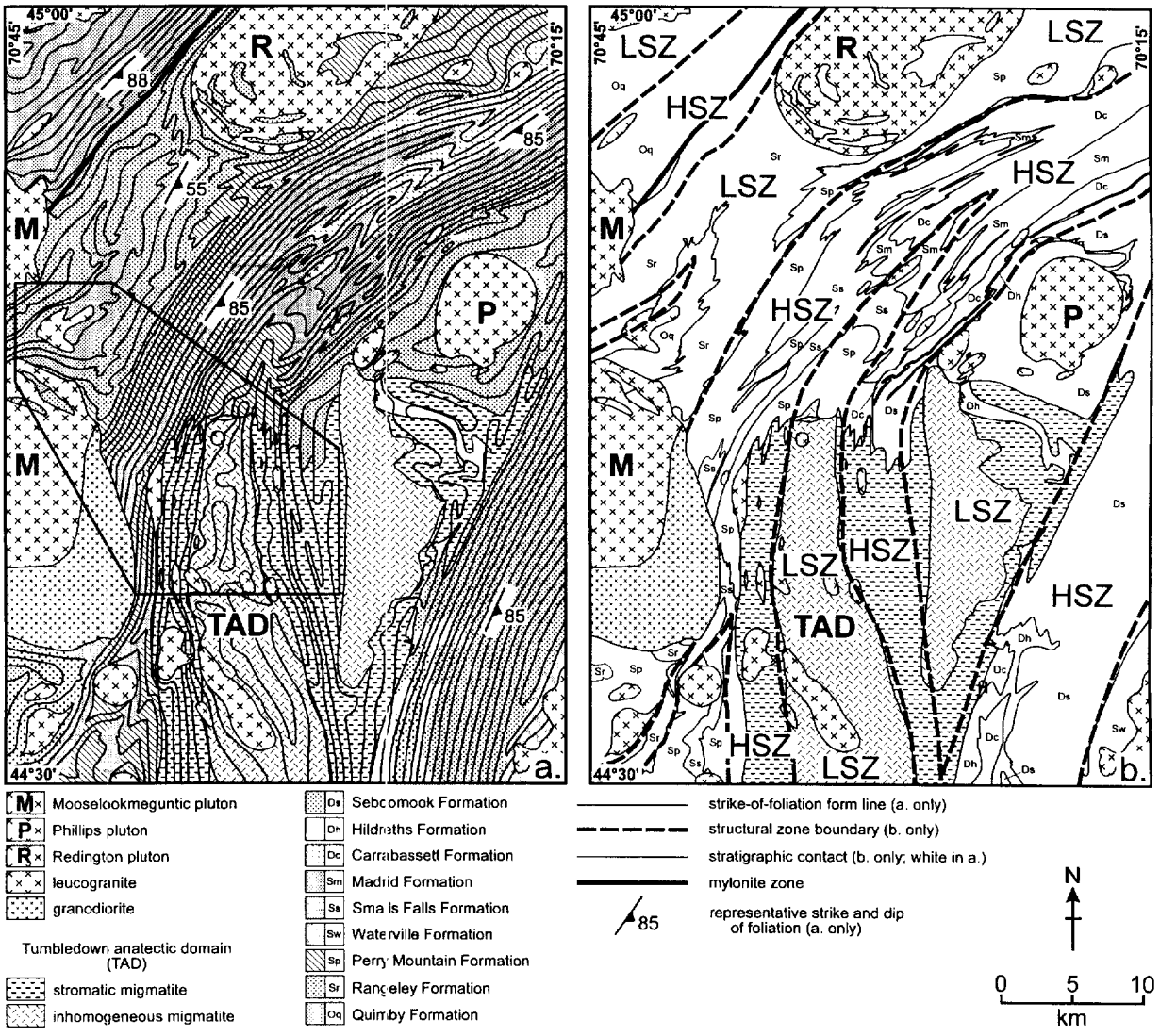

Fig. 5. (a) Simplified geological and foliation form line map of the Tumbledown Mountain area, west-central Maine (Tumbledown Mountain approximately at the center of the map). The area outlined encloses the detailed map in Fig. 6(a & b). The strike of the foliation form lines are superimposed on stratigraphic formations. The closeness of form lines indicates general dip (closely spaced lines denote steeply dipping foliation, widely spaced lines denote moderately dipping foliation). High-strain zones are expressed on the map by parallelism of strike of foliation form lines. This map is based on new field data, and interpreted from extant data of Moench (1971) and Moench and Hildreth (1976). (b) Although stratigraphic units described by Moench (1970) do not need to be distinguished in detail for the purposes of this paper, notice the coincidence of boundaries between higher strain zones and zones of lower strain with formation contacts. Granite plutons are found in the areas of lower strain (Redington pluton and Phillips pluton) or cutting higher strain zones (Mooselookmeguntic pluton); inhomogeneous migmatite of the Tumbledown anatectic domain (TAD) lies within zones of lower strain, whereas stromatic migmatite is located on either side, mostly coinciding with the higher strain zones.

completely ceased. In contrast, the TAD and some granite plutons are found in zones of lower strain (Fig. 5b). The TAD (Fig. 5b) includes anatectic migmatites (Fig. 8) with variable leucosome proportions, from stromatic migmatite (Fig. 7b & c) to schlieric inhomogeneous migmatite (Fig. 7e) and discrete bodies of schlieric granite (Fig. 7f). Foliation and leucosomes in stromatic migmatites are consistently parallel to the TAD margin, and the foliation in surrounding rocks. Sheets of leucogranite with biotite-rich schlieren or laminae occur within the stromatic migmatites; generally they are concordant with foliation in the surrounding stromatic migmatites (Fig. 7c), although locally the sheet margins may cut across the foliation at a small angle. We interpret these sheets to occur in tensile or dilatant shear fractures (Brown and Solar, in review). Flow foliation within these sheets is sometimes present, in which cases it is parallel to the walls to suggest laminar flow during migration of the granite. Occasional schlieren structure exhibits asymmetry consistent with dextral displacement (Fig. 7d).

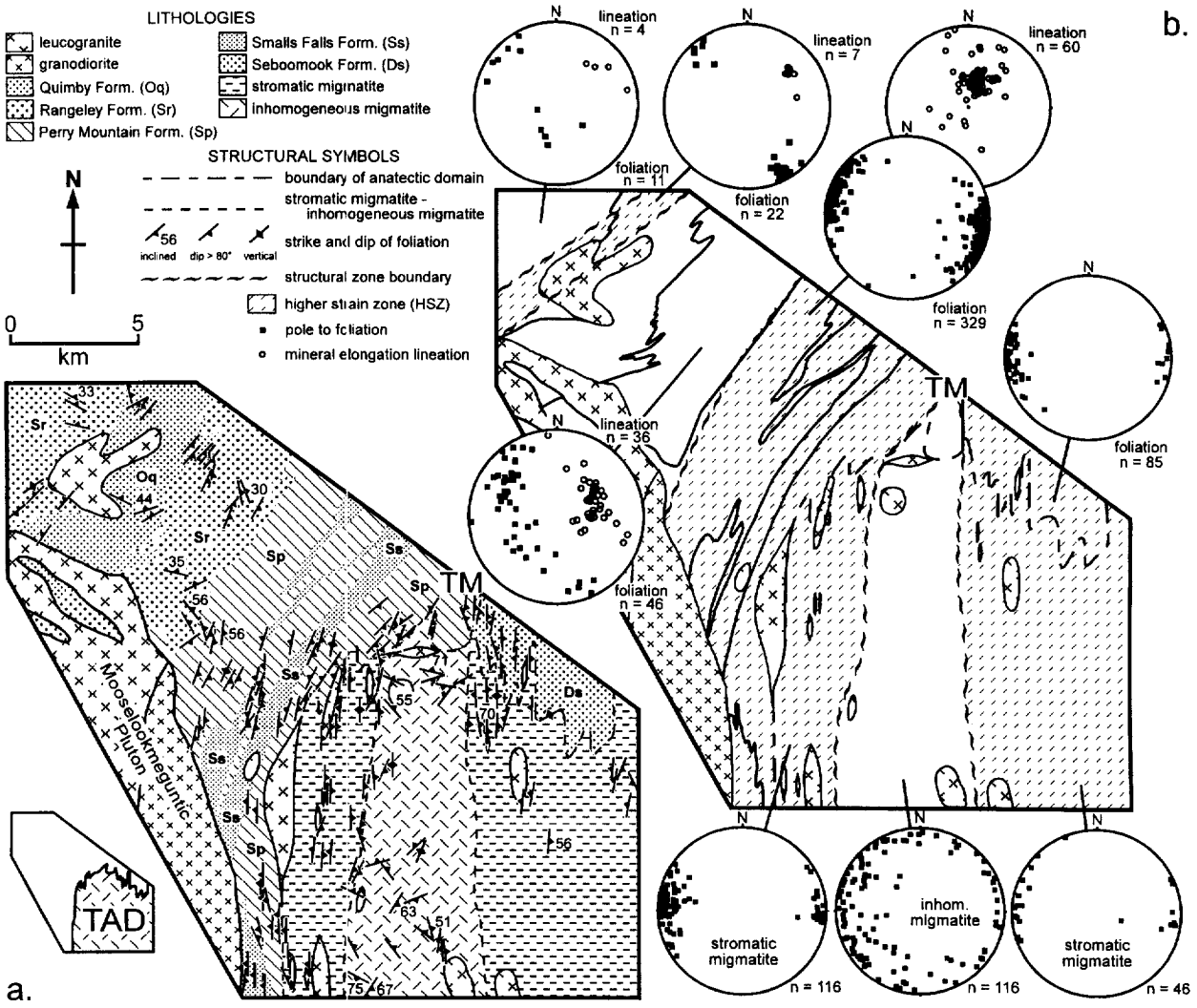

Fig. 6. (a) Detailed lithological and structural map of the Tumbledown Mountain area. For clarity, strike and dip symbols are representative examples taken from up to 10 closely spaced measurements of foliation with similar orientations in large or densely spaced outcrops. (b) Summary of structural data, stereograms are lower-hemisphere (Schmidt) projections of poles to foliation (black squares) and mineral elongation lineations (open circles). TM represents Tumbledown Mountain.

Narrow transition zones (Fig. 5; structural zone boundaries) separate stromatic migmatite (exclusively inside higher strain zones; Fig. 7b & c) and inhomogeneous migmatite (Fig. 7f) into separate domains (Figs 4b & 5). The transition zones are composed of stromatic to schlieric migmatite in which the stromatic type occurs as shear-bounded blocks within schlieric migmatite (Fig. 7e). Because the transition zone separates stromatic migmatite from schlieric migmatite, we suggest it formed by disruption during unstable flow at the edge of a higher strain zone where it impinged on a lower strain zone that contained a higher vol.% melt.

The anastomosing pattern of higher strain zones that surround zones of lower strain is an example of self-organization in a non-equilibrium system leading to development of dissipative structure. This structure represents the percolation network through which granite melt migrated from upstream sources deeper in the crust along higher strain zones into zones of lower strain at the downstream end of architecture produced by the transpressional deformation. Granites emplaced within high-strain zones generally do not exhibit *C–S* fabrics, which suggests crystallization occurred as the rate of deformation waned. Although the granites do not exhibit evidence of significant subsolidus strain, exactly how much strain was accommodated by flow in granite at the magmatic stage is uncertain. Upward transfer of granite melt was arrested at the brittle–plastic transition and melt became emplaced as plutons by inflation during flow into lateral fractures (Brown and Solar, in review).

Summary

Transfer of granite melt through the crust in west-central Maine occurred within a crustal-scale shear-zone system that accommodated dextral transpression. Con-

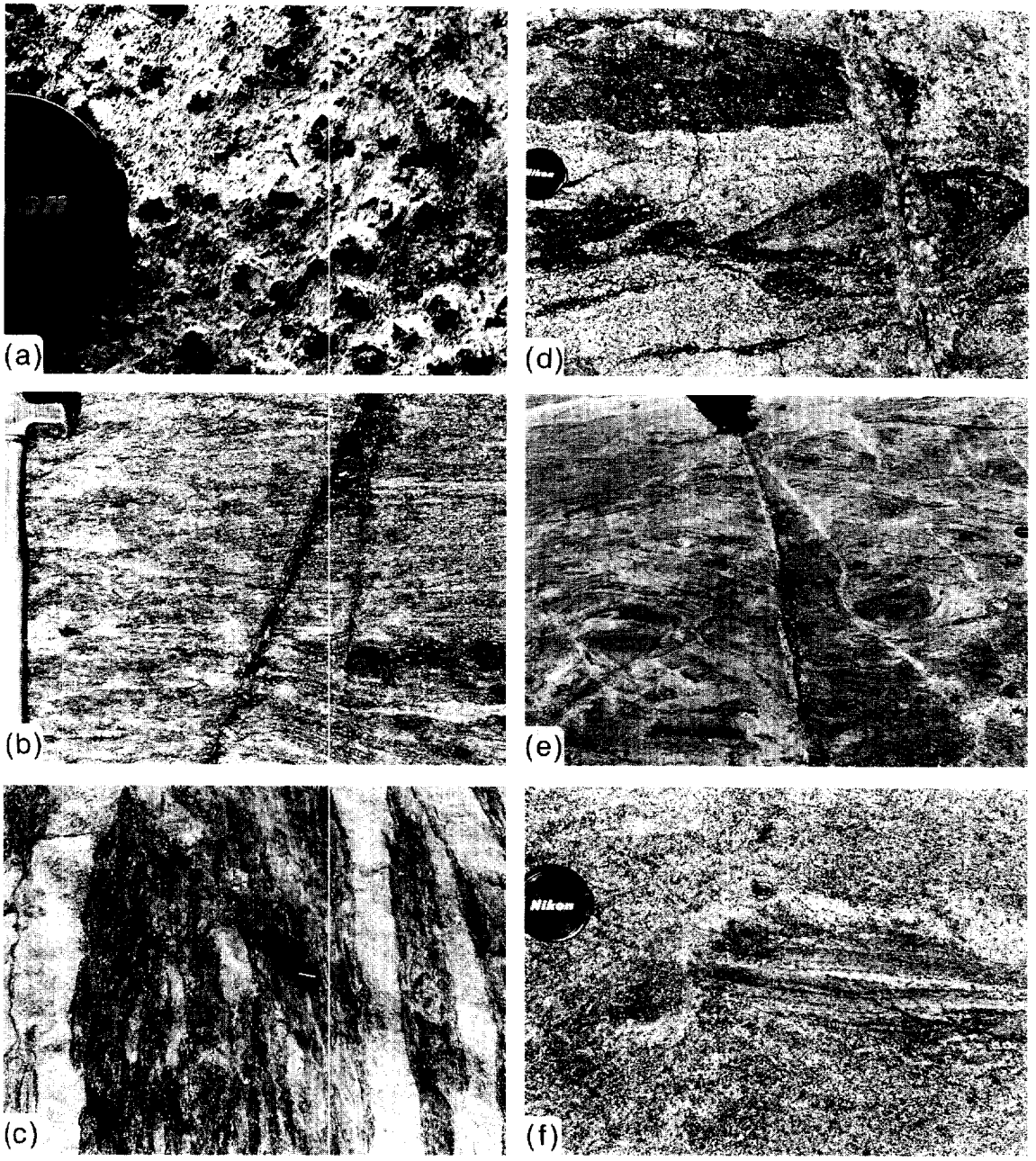

Fig. 7. Examples of relations from the Central Maine belt, west-central Maine, U.S.A. (a) Staurolite euhedra in subvertical foliation in pelitic schists (Perry Mountain Formation, foliation-parallel view looking east-southeast), the lineation is defined by elongate muscovite and biotite 'fish', locality in the high-strain zone. (b) Stromatic migmatite, locality in the high-strain zone, to illustrate pervasively parallel leucosome, melanosome and mesosome foliation (steeply E-dipping, north is to the right). (c) Centimeter-scale, sub-vertical, granite sheets in the stromatic migmatite unit shown in (b) (steeply E-dipping, view to the south), locality in the high-strain zone. (d) Flow foliation in meter-scale, subvertical, schlieric-granite sheet in stromatic migmatite close to the outcrop shown in (c), locality in the high-strain zone. Note the asymmetry exhibited by the schlieren structure, which is consistent with a component of dextral displacement. (e) Foliated inhomogeneous migmatite at the eastern margin of a high-strain zone (north is to the left). Notice the relatively higher vol.% leucosome and flow foliation defined by the schlieren structure, in comparison with the stromatic migmatite shown in (b) and (c). (f) Schlieric granite, part of the inhomogeneous migmatite unit, Tumbledown anatectic domain.

tractional thickening of the CMB sedimentary basin by homogeneous distributed shear was followed by thermal relaxation to generate high-T–low-P metamorphism leading to crustal anatexis. Relative displacement of rock units was steeply oblique-reverse at the present level of erosion, along the steeply plunging mineral elongation lineation preserved in the non-anatectic rocks; we presume the system soles in the lower–middle crust at depth as implied by modelling of geophysical data (Stewart *et al.*, 1992). The mineral elongation lineation developed syntectonically. Thus, metamorphism was dynamic and synchronous with granite melt migration. Strain became localized at rheological heterogeneities, which were controlled by melting superimposed

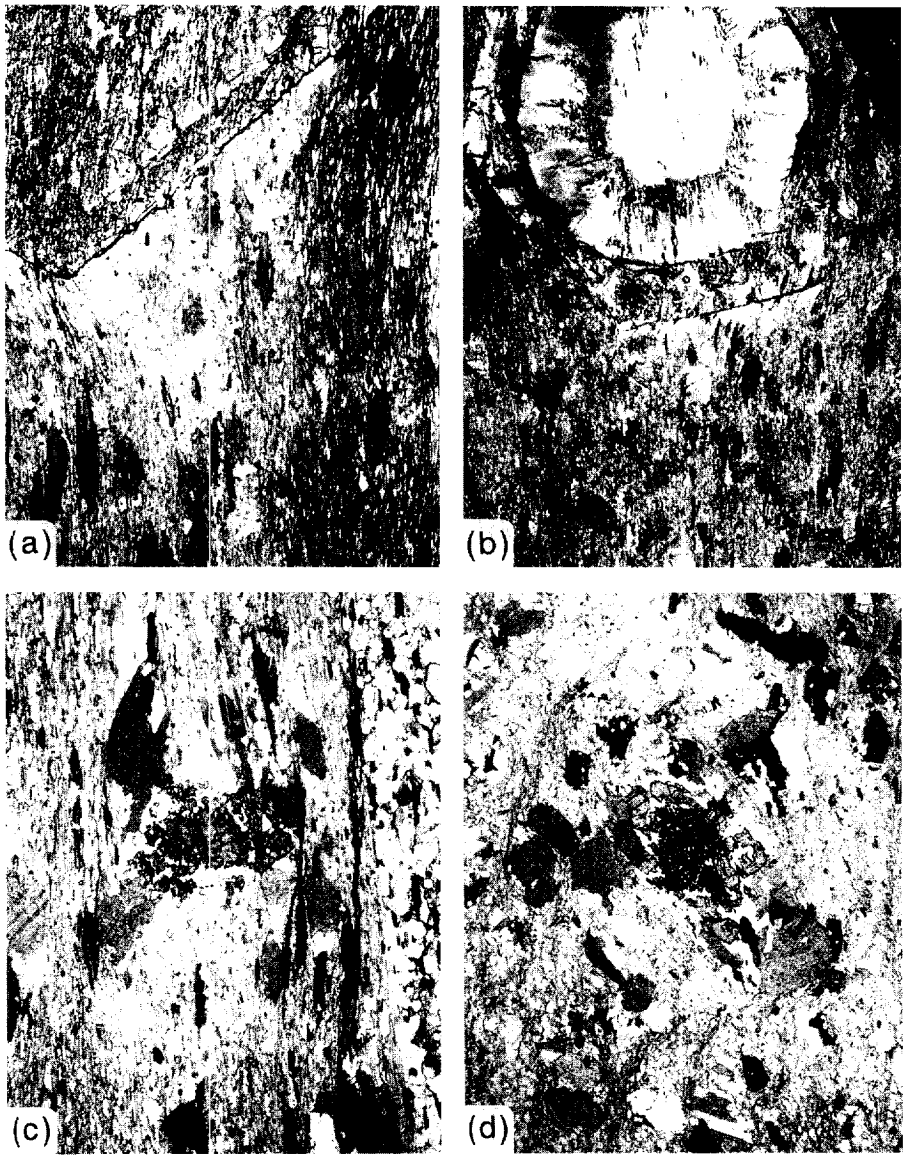

Fig. 8. Pairs of photomicrographs (plane-polarized light; long dimension is 7 mm) of the microstructure in mutually perpendicular thin sections oriented with respect to tectonic fabric, cut from pelite–psammite metasedimentary rocks (quartz + muscovite + biotite + garnet + staurolite + chlorite + andalusite) from high (a and b) and low (c and d) strain zones, Central Maine belt, west-central Maine, U.S.A. (a) An example of a high-strain zone microstructure in thin section cut parallel to the mineral elongation lineation and perpendicular to foliation (Coos Canyon, Byron, Maine). Notice the strongly developed fabric and the pressure shadow tail at the euhedral edge to a large staurolite porphyroblast. (b) Microstructure in thin section from the same sample as (a), cut perpendicular to both mineral elongation lineation and foliation. Notice the strongly developed fabric similar to (a) but notice also that the euhedral staurolite porphyroblast has only a weakly developed pressure shadow tail in contrast to (a). The strongly developed foliation traces and pressure shadow tails in both (a) and (b) are consistent with an interpretation that the fabric records flattening strain. The strongly developed mineral elongation lineation suggests plastic deformation was close to plane strain. (c) An example of a lower strain zone microstructure in thin section cut parallel to mineral elongation lineation and perpendicular to foliation (Swift River, Byron, Maine). Notice the strongly developed fabric in this view, and the parallelism of tectonic fabric with the pelite–psammite contact (relict bedding surface; right). Also notice the significant difference in recorded strain between pelite and psammite quartz, which suggests strain partitioning into the pelite. (d) Microstructure in thin section from the same sample as (c), cut perpendicular to mineral elongation lineation and foliation. The weakly developed foliation traces and equant porphyroblasts of staurolite and biotite in this orientation in contrast to (c) are consistent with an interpretation that the fabric records constrictional strain.

on original lithological differences between stratigraphic formations in the anatectic domain. The occurrence of lower vol.% leucosome within higher strain residual stromatic migmatites suggests that granite melt has been lost from higher strain zones. This is consistent with flattening strain. Melt flow is inferred to have been essentially parallel to the maximum principal finite elongation direction in the plane of flattening, into areas of lower strain at shallower levels in the crust, consistent with constrictional strain. Granite arrested and crystallized during ascent within high-strain zones exhibits flow foliation but has not developed *C–S* fabrics.

Maximum melt production probably occurred during the peak-*T* part of the *P–T* history. This is likely to

represent the time of maximum weakening in the higher grade rocks, the period of highest melt transfer rate and the time of maximum deformation rate. Once cooling along the retrograde P–T path began, deformation rates are likely to have declined and strain became progressively more localized. This thermal–rheological evolution occurred both in time and space. Thus, a melting front and shear-zone system propagated upward and outward from the orogenic core, and was followed by a contracting cooling front in the reverse sense. Consequently, the depth to the brittle–plastic transition in the crust first decreased and then increased during the orogenic cycle.

DISCUSSION: DISSIPATIVE STRUCTURE AND MELT MIGRATION

Variations in differential stress must be reflected in pressure gradients at the same scale. For the case of actively deforming dilatant high-strain zones, fluid migration may be enhanced by an increase in the P gradient and enabled by an increase in dilatancy. Dilatancy represents an increase in porosity that will enhance the possibility of fluid flow, if permeability increases with porosity (Ord, 1990). Both dilatancy and enhanced permeabilities are common features of active shear-zone systems in the crust, evidenced by petrological and geochemical studies of natural shear-zone systems (Hobbs *et al.*, 1990; Tullis *et al.*, 1996), and supported by modelling (Ord, 1990; O'Hara, 1994; Ord and Oliver, 1997). Although the fluid flow properties and the permeability structure of shear-zone systems are not adequately characterized, quasi-steady-state permeabilities are implied that reflect a balance between porosity creation (e.g. by volume change due to melting, grain-boundary sliding and melt-induced cataclasis) and porosity reduction (e.g. by shear-induced compaction through grain-boundary sliding and melt-assisted grain-boundary diffusive mass transfer). Balance is achieved by the tendency for melt pressure to remain close to lithostatic, which results in grain-scale dilatancy-driven fluid pumping (Brown, 1994).

We suggest that melt may be moved along high-strain zones parallel to the maximum principal finite elongation direction (assumed to be materialized by the mineral elongation lineation). Besides changes in permeability induced by deformation (e.g. Cox *et al.*, 1987; Zhang *et al.*, 1994), we consider deformation-induced dilatancy to be the principal mechanism that pumps melt along foliation planes parallel to the mineral elongation lineation (cf. Ord and Oliver, 1997). Ord and Oliver (1997) estimate that the influence of plastic dilatancy upon fluid flow continues for at least as long as the plastic deformation continues before decay sets in. Thus, it can be expected to last throughout the deformational regime of an orogenic event. Because deformation-induced dilatancy will influence melt pressure and, in turn, the effective stress responsible for continued deformation, a feedback relation is activated that couples melt behavior with deformation. The feedback relation between increasing melt fraction, localization of non-coaxial strain into leucosomes and migration of melt to accommodate coaxial strain reflects inhomogeneous deformation at the mesoscale repeated at the macroscopic scale. Thus, at all scales the deformation becomes partitioned into zones of higher and lower strain. We postulate that a crustal-scale network is formed by interconnection of macroscopic high-strain zones, and melt flow will focus into anastomosing high-strain zones that surround lens-shaped zones of lower strain as strain becomes localized. Put another way, self-organization of the system (the orogenic system) leads to the appearance of a dissipative structure (the shear-zone architecture) by amplification of appropriate fluctuations (due to melting). The architecture that develops in response to partitioning of strain in orogenic belts is a first-order control on the transfer of melt through the mid-crust and the location of plutons in the upper crust. The relationship between deformation and melt flow, however, may be counterintuitive.

Percolative melt flow through shear-zone systems is likely to occur only during active deformation (O'Hara, 1994; Ord and Oliver, 1997), but build-up of melt pressure will cause melt-enhanced embrittlement, tensile or dilatant shear fracturing, and channelized flow (Davidson *et al.*, 1994; Brown and Solar, in review). Thus, it is the feedback relations between rates of strain, melt production and melt flow within the crustal-scale shear-zone system that determine whether melt flow is percolative or channelized. The type of shear-zone system (transcurrent, normal, reverse or oblique) will control the vector of percolative melt flow, because anisotropy of permeability is related to strain and the orientation of the strain ellipsoid is different in each type of shear-zone system. The strength of crustal materials depends upon the orientation of fabric anisotropy with respect to the imposed non-hydrostatic stress field. The result is a competition between the imposed non-hydrostatic stress field and tectonically induced melt pressure, structural control over the transfer of melt along dilational high-strain zones, and buoyancy forces acting on the melt.

GENERAL MODEL

During active deformation in an ideal transcurrent shear-zone system with horizontal maximum principal finite elongation direction (Fig. 9A), percolative flow will tend to be horizontal so that melt effectively will be stagnant. Consequently, melt pressure builds up leading to melt-enhanced embrittlement (Davidson *et al.*, 1994) and channelized transfer in subvertical foliation-parallel tensile or dilatant shear fractures concurrently with active deformation. At this stage, both tectonically induced melt pressure and buoyancy contribute to the driving force for magma ascent. Granites emplaced in the shear-zone system during ascent develop C–S fabrics as

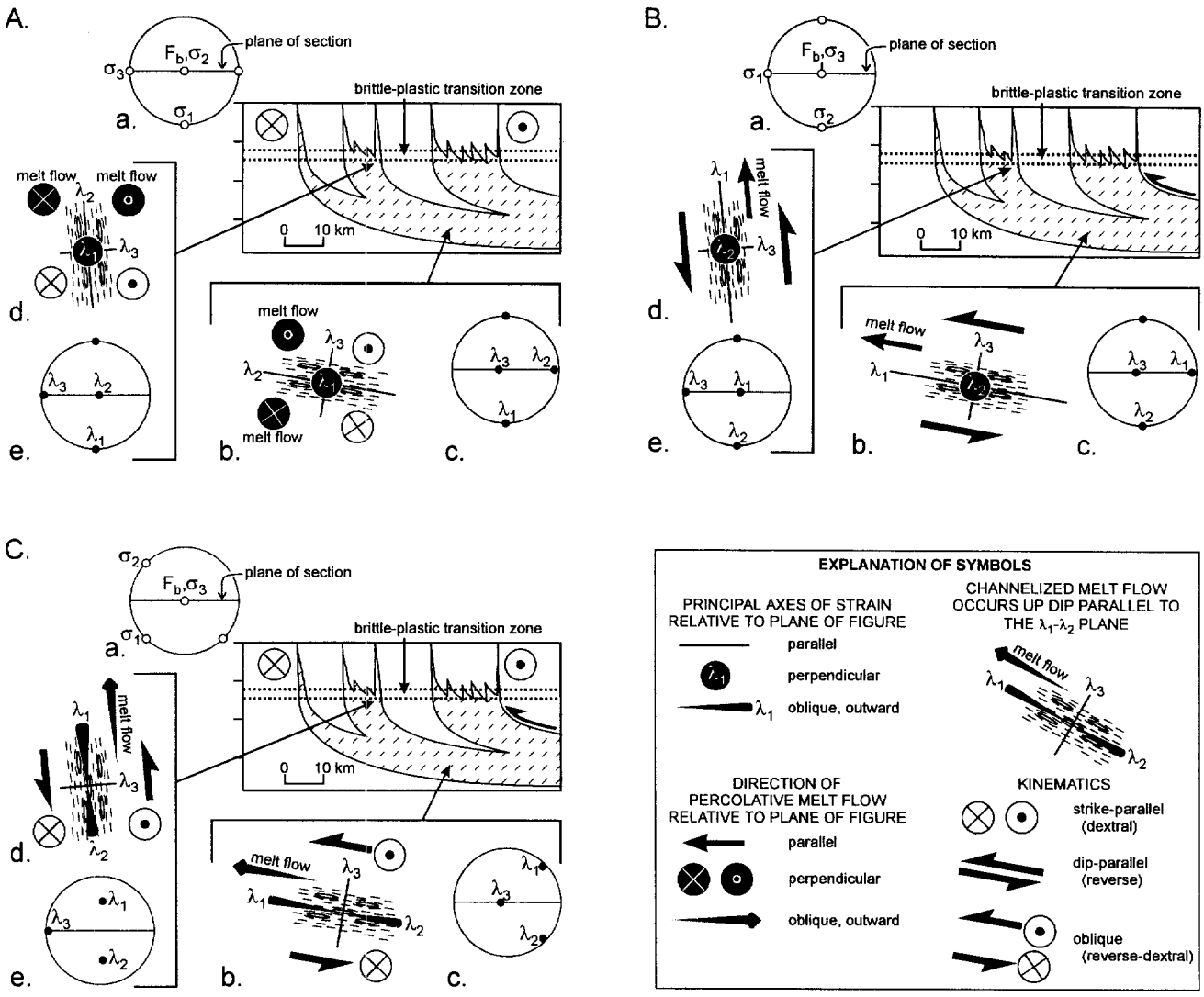

Fig. 9. Schematic cross-sections of: (A) an ideal transcurrent shear-zone system (with horizontal maximum principal finite elongation direction; this example is dextral); (B) an ideal reverse shear-zone system (with down-dip maximum principal finite elongation direction); and (C) an oblique-slip shear-zone system (in which the maximum principal finite elongation direction has a pitch of 45° into the plane of section on the plane of flattening; this example is dextral-reverse). Cross-sections are drawn without vertical exaggeration perpendicular to the principal plane of flattening. The short diagonal ornament corresponds to high-strain zones that surround zones of lower strain (unornamented). In each figure: (a) is a lower-hemisphere (Schmidt) projection of the far-field stresses with $\sigma_1 > \sigma_2 > \sigma_3$ and F_b the force due to buoyancy; (b) is the relationship between tectonic structures (short dashes are the intersection of foliation with the plane of the section, and thin ellipses are melt batches), principal finite elongation directions (where $\lambda_1 > \lambda_2 > \lambda_3$), kinematics and melt flow in the shallowly dipping sole of the system; (c) is a lower-hemisphere (Schmidt) projection of the principal finite elongation directions in the shallowly dipping sole of the system; (d) is the relationship between tectonic structures (short dashes are the intersection of foliation with the plane of the section, and thin ellipses are melt batches), principal finite elongation directions (where $\lambda_1 > \lambda_2 > \lambda_3$), kinematics and melt flow in the steeply dipping part of the system; (e) is a lower-hemisphere (Schmidt) projection of the principal finite elongation directions in the steeply dipping part of the system.

strain concentrates in them during crystallization and subsolidus cooling. In an ideal reverse shear-zone system with down-dip maximum principal finite elongation direction (Fig. 9B), although percolative flow will be subhorizontal in the listric sole this flow becomes steep to subvertical in the middle–upper crust. Melt transfer upward through the crust by percolative flow will be effective in these systems in comparison with transcurrent systems because buoyancy forces contribute significantly to the driving force for melt flow (Brown and Solar, in review) along the maximum principal finite elongation direction (up-plunge along the mineral elongation lineation). During waning deformation in these systems, however, build-up of melt pressure leads to melt-enhanced embrittlement and channelized transfer of melt in subvertical foliation-parallel tensile or dilatant shear fractures (Brown and Solar, in review). Here, granites emplaced in the shear-zone system during ascent do not develop *C–S* fabrics during crystallization and subsolidus cooling. The general case lies between these two ideal cases (Fig. 9C) and whether the resultant melt flow history is closer to the transcurrent or reverse

end-member will be determined by the obliquity of the slip vector.

We relate our specific examples to this general model as follows. For the example of the St. Malo migmatite belt and the Mancellian granites, this is a case that lies close to the ideal transcurrent shear-zone system end-member. Granites emplaced in transcurrent high-strain zones marginal to the St. Malo migmatite belt developed *C–S* fabrics as strain concentrated in them during persistent deformation synchronous with crystallization and subsolidus cooling. Thus, the granite magma is interpreted to have been arrested during ascent through an actively deforming shear-zone system. For the example of the Central Maine belt, this is a case that lies close to the ideal reverse shear-zone system end-member. Granites emplaced in high-strain zones in this shear-zone system did not develop *C–S* fabrics during crystallization and subsolidus cooling, which implies late syntectonic ascent and emplacement as deformation waned.

CONCLUSIONS

(1) As orogenic systems are driven far from equilibrium, amplification of fluctuations within the system leads to the appearance of dissipative structure by self-organization. Crustal-scale shear-zone systems are an example of dissipative structure developed in response to rheological heterogeneities in the crust, particularly the presence of melt, and the imposed far-field tectonic stresses. The resulting finite-strain field is heterogeneous, large variations in strain are possible and complex kinematic patterns may occur.

(2) During crustal-scale inhomogeneous flow, initial melting generates instabilities that localize strain and control the architecture of the orogenic system. Although the morphology of the latter may evolve during orogenesis, its basic structure will not change significantly. Movement of melt out of the anatectic zone is an important mechanism by which the crust below the brittle–plastic transition accommodates strain. Thus, granite melt migrates through the crust within crustal-scale shear-zone systems. At high strains this movement is essentially parallel to the maximum principal finite elongation direction, manifested by the mineral elongation lineation. Channelized transfer of granite melt batches in tensile or dilatant shear fractures from sources at deeper levels in the crust to pluton sinks at shallower levels is driven by a combination of buoyancy forces and tectonically induced melt pressure, but the pathways for both percolative and channelized melt flow are controlled by the pattern of tectonic structures. This is an example of a feedback relation in which interactions between rates of strain, melt production and percolative flow determine whether build-up of melt pressure is sufficient to enable fracturing and channelized transfer of melt in batches. Once a dissipative structure is generated by self-organization, zones of lower strain into which granite melt may accumulate essentially are pre-determined.

Acknowledgements—We acknowledge discussions with colleagues too numerous to mention individually, including members of the Laboratory for Crustal Petrology and the Maine Geological Survey, and with participants in NEIGC Field Trip C5 in September of 1996. Comments on an earlier manuscript from Scott E. Johnson and Edward W. Sawyer, and journal reviews by J. Luc Bouchez and Stefan Schmid enabled us to focus better the content of this paper; we are grateful to J. Luc Bouchez for numerous suggestions that helped us to express our ideas with greater clarity. However, we take responsibility for those infelicities that remain. Chuck Guidotti and E-an Zen introduced us to the geology of west-central Maine, and we thank them for continuing interest in and comments on our work. This research was supported in part by the Department of Geology, University of Maryland and the Geological Society of America Research Grant Program. We thank Jeanne Martin for skilled wordprocessing support and her tolerance of the senior author.

REFERENCES

Allen, T. T. (1996) Petrology and stable isotope systematics of migmatites in Pinkham Notch New Hampshire. In *Guidebook to Fieldtrips in Northern New Hampshire and Adjacent Regions of Maine and Vermont, New England Intercollegiate Geological Conference*, pp. 279–298. 88th Annual Meeting, Trip C2.

Berthé, D., Choukroune, P. and Jegouzo, P. (1979) Orthogneiss, mylonite and non-coaxial deformation of granites: The example of the South Armorican Shear Zone. *Journal of Structural Geology* **1**, 31–41.

Brodie, K. (1995) The development of orientated simplectites during deformation. *Journal of Metamorphic Geology* **13**, 499–508.

Brown, M. (1974) The petrogenesis of the St. Malo Migmatite Belt, north-eastern Brittany, France. Ph.D. thesis, University of Keele, Staffordshire, UK.

Brown, M. (1978) The tectonic evolution of the Precambrian rocks of the St. Malo region, Armorican Massif, France. *Precambrian Research* **6**, 1–21.

Brown, M. (1979) The petrogenesis of the St. Malo Migmatite Belt, Armorican Massif, France, with particular reference to the diatexites. *Neues Jahrbuch fur Mineralogie Abhandlungen* **135**, 48–74.

Brown, M. (1994) The generation, segregation, ascent and emplacement of granite magma. *Earth Science Reviews* **36**, 83–130.

Brown, M. (1995) Late-Precambrian geodynamic evolution of the Armorican Segment of the Cadomian Belt (France): Distortion of an active continental margin during south-west directed convergence and subduction of a bathymetric high. *Géologie de la France* **3**, 3–22.

Brown, M., Averkin, Y., McLellan, E. and Sawyer, E. (1995) Melt segregation in migmatites. *Journal of Geophysical Research* **100**, 15655–15679.

Brown, M. and Dallmeyer, R. D. (1996) Rapid Variscan exhumation and role of magma in core complex formation: Southern Brittany metamorphic belt, France. *Journal of Metamorphic Geology* **14**, 361–379.

Brown, M. and D'Lemos, R. S. (1991) The Cadomian granites of Mancellia, north-east Armorican massif of France: Relationship to the St. Malo Migmatite Belt, petrogenesis and tectonic setting. *Precambrian Research* **51**, 393–427.

Brown, M., Power, G. M., Topley, C. G. and D'Lemos, R. S. (1990) Cadomian magmatism in the North Armorican Massif. In *The Cadomian Orogeny*, eds R. S. D'Lemos, R. A. Strachan and C. G. Topley, pp. 181–213. Geological Society of London Special Publication **51**.

Brown, M. and Rushmer, T. (1997) The role of deformation in the movement of granitic melt: Views from the laboratory and the field. In *Deformation-enhanced Melt Segregation and Metamorphic Fluid Transport*, ed. M. Holness. The Mineralogical Society Series. Chapman and Hall, London.

Brown, M. and Solar, G. S. (in review) Granite ascent and emplacement in contractional orogenic belts. *Journal of Structural Geology*.

Brun, J.-P. and Balé, P. (1990) Cadomian tectonics in Northern

Brittany. In *The Cadomian Orogeny*, eds R. S. D'Lemos, R. A. Strachan and C. G. Topley, pp. 95–114. Geological Society of London Special Publication **51**.

Brun, J.-P., Guennoc, P. and ARMOR Group (1997) The Cadomian crust of Northern Brittany: 3D geological and geophysical modelling (Geofrance 3D Program). *Terra Nova* **9**, Abstract Supplement No. 1, 110.

Casey, M. (1980) Mechanics of shear zones in isotropic dilatant materials. *Journal of Structural Geology* **2**, 143–147.

Chamberlain, C. P. and Robinson, P. (1989) *Styles of Metamorphism With Depth in the Central Acadian High New England.* Department of Geology and Geography, University of Massachusetts, Amherst, Contribution 63.

Chamberlain, C. P. and Sonder, L. J. (1990) Heat-producing elements and the thermal and baric patterns of metamorphic belts. *Science* **250**, 763–769.

Cogné, J. and Wright, A. E. (1980) Orogène cadomien. In *26th International Geological Congress, Paris*, pp. 29–55. Mémoires Bureau de Recherches Géologiques et Minières **108**.

Cox, S. F., Etheridge, M. A. and Wall, V. J (1987) The role of fluids in syntectonic mass transport, and the localization of metamorphic vein-type ore deposits. *Ore Geology Reviews* **2**, 65–86.

Dallmeyer, R. D., Brown, M., D'Lemos, R. S. and Strachan, R. A. (1993) Variable Variscan thermal rejuvenation in the St. Malo region, Cadomian Orogen, France: Evidence from $^{40}Ar/^{39}Ar$ mineral ages. *Journal of Metamorphic Geology* **11**, 137–154.

Davidson, C., Hollister, L. S. and Schmid, S. M. (1992) Role of melt in the formation of a deep-crustal compressive shear zone: The MacLaren Glacier metamorphic belt, South Central Alaska. *Tectonics* **11**, 348–359.

Davidson, C., Schmid, S. M. and Hollister, L. S. (1994) Role of melt during deformation in the deep crust. *Terra Nova* **6**, 133–142.

DeYoreo, J. J., Lux, D. R., Guidotti, C. V., Decker, E. R. and Osberg, P. H. (1989) The Acadian thermal history of western Maine. *Journal of Metamorphic Geology* **7**, 169–190.

D'Lemos, R. S. and Brown, M. (1993) Sm–Nd isotope characteristics of Late Cadomian granite magmatism in Northern France and the Channel Islands. *Geological Magazine* **130**, 797–804.

D'Lemos, R. S., Brown, M. and Strachan, R. A. (1992) Granite magma generation, ascent and emplacement within a transpressional orogen. *Journal of the Geological Society of London* **149**, 487–490.

Dupret, L., Dissler, E., Doré, F., Gresselin F. and Le Gall, J. (1990) Cadomian geodynamic evolution of the northeastern Armorican Massif (Normandy and Maine). In *The Cadomian Orogeny*, eds R. S. D'Lemos, R. A. Strachan and C. G. Topley, pp. 115–131. Geological Society of London Special Publication **51**.

Eusden, J. D. and Barreiro, B. (1988) The timing of peak high-grade metamorphism in central-eastern New England. *Maritime Sedimentation and Atlantic Geology* **24**, 241–255.

Gapais, D. (1989) Shear structures within deformed granites: Mechanical and thermal indicators. *Geology* **17**, 1144–1147.

Gapais, D. and Balé, P. (1990) Shear zone pattern and granite emplacement within a Cadomian sinistral wrench zone at St. Cast, N. Brittany. In *The Cadomian Orogeny*, eds R. S. D'Lemos, R. A. Strachan and C. G. Topley, pp. 169–179. Geological Society of London Special Publication **51**.

Getty, S. R. and Gromet, L. P. (1992) Geochronological constraints on ductile deformation, crustal extension, and doming about a basement–cover boundary, New England Appalachians. *American Journal of Science* **292**, 359–397.

Graviou, P. F. and Auvray, B. (1985) Caracterisation pétrographique et géochimique des granitoïdes cadomiens du domaine nord-armoricain: implications géodynamiques. *Comptes rendus de l'Academie des Sciences, Paris* **303**, 315–318.

Graviou, P., Peucat, J.-J., Auvray, B. and Vidal, P. (1988) L'orogènese cadomienne dans le nord du massif armoricain: pétrologie et géochronologie. *Hercynica* **IV**, 1–13.

Guidotti, C. V. (1989) Metamorphism in Maine: an overview. In *Studies in Maine Geology, Igneous and Metamorphic Geology*, eds R. D. Tucker and R. G. Marvinney, Vol. 3, pp. 1–19. Maine Department of Conservation.

Hatch, N. L., Moench, R. H. and Lyons, J. B. (1983) Silurian–lower Devonian stratigraphy of eastern and south-central New Hampshire: Extensions from western Maine. *American Journal of Science* **283**, 739–761.

Hobbs, B. E., Mühlhaus, H.-B. and Ord, A. (1990) Instability, softening and localization of deformation. In *Deformation Mechanisms, Rheology and Tectonics*, eds R. J. Knipe and E. H. Rutter, pp. 143–165. Geological Society of London Special Publication London **54**.

Hollister, L. S. (1993) The role of melt in the uplift and exhumation of orogenic belts. *Chemical Geology* **108**, 31–48.

Hollister, L. S. and Crawford, M. L. (1986) Melt-enhanced deformation: A major tectonic process. *Geology* **14**, 558–561.

Holness, M. B. (1997) The permeability of non-deforming rock. In *Deformation-enhanced Melt Segregation and Metamorphic Fluid Transport*, ed. M. Holness. The Mineralogical Society Series. Chapman and Hall, London.

Hutton, D. H. W. and Reavy, R. J. (1992) Strike-slip tectonics and granite petrogenesis. *Tectonics* **11**, 960–967.

Ingram, G. M. and Hutton, D. H. W. (1994) The Great Tonalite Sill: Emplacement into a contractional shear zone and implications for Late Cretaceous to early Eocene tectonics in southeastern Alaska and British Columbia. *Bulletin of the Geological Society of America* **106**, 715–728.

Laporte, D. and Watson, E. B. (1995) Experimental and theoretical constraints on melt distribution in crustal sources: The effect of crystalline anisotropy on melt interconnectivity. *Chemical Geology* **124**, 161–184.

Laporte, D., Rapaille, C. and Provost, A. (1997) Wetting angles, equilibrium melt geometry, and the permeability threshold of partially molten crustal protoliths. In *Granite: From Melt Segregation to Emplacement Fabrics*, eds J.-L. Bouchez, D. Hutton and W. E. Stephens. Kluwer Academic, Amsterdam.

Lathrop, A. S., Blum, J. D. and Chamberlain, C. P. (1994) Isotopic evidence for closed-system anatexis at midcrustal levels; an example from the Acadian Appalachians of New England. *Journal of Geophysical Research* **99**, 9453–9468.

Moecher, D. P. and Wintsch, R. P. (1994) Deformation-induced reconstitution and local resetting of mineral equilibria in polymetamorphic gneisses: Tectonic and metamorphic implications. *Journal of Metamorphic Geology* **12**, 523–538.

Moench, R. H. (1970) Premetamorphic down-to-basin faulting, folding, and tectonic dewatering, Rangeley area, western Maine. *Bulletin of the Geological Society of America* **81**, 1463–1496.

Moench, R. H. (1971) *Geologic Map of the Rangeley and Phillips Quadrangles, Franklin and Oxford Counties, Maine.* U.S. Geological Survey Miscellaneous Investigations Map **I-605**.

Moench, R. H. and Hildreth, C. T. (1976) *Geologic Map of the Rumford Quadrangle, Oxford and Franklin Counties, Maine.* U.S. Geological Survey Quadrangle Map **GQ-1272**.

Nelson, K. D. (1996) Partially molten middle crust beneath southern Tibet: Synthesis of project INDEPTH results. *Nature* **274**, 1684–1688.

Neves, S. P., Vauchez, A. and Archanjo, C. J. (1996) Shear zone-controlled magma emplacement or magma-assisted nucleation of shear zones? Insights from northeast Brazil. *Tectonophysics* **262**, 349–364.

Nicolis, G. and Prigogine, I. (1977) *Self-organization in Nonequilibrium Systems. From Dissipative Structures to Order Through Fluctuations.* John Wiley & Sons, New York.

O'Hara, K. D. (1994) Fluid–rock interaction in crustal shear zones: A directed percolation approach. *Geology* **22**, 843–846.

Ord, A. (1990) Mechanical controls on dilatant shear zones. In *Deformation Mechanisms, Rheology and Tectonics*, eds R. J. Knipe and E. H. Rutter, pp. 183–192. Geological Society of London Special Publication **54**.

Ord, A. and Oliver, N. H. S. (1997) Mechanical controls on fluid flow during regional metamorphism: some numerical models. *Journal of Metamorphic Geology* **15**, 345–359.

Ortoleva, P. J. (1994) *Geochemical Self-organization.* Oxford University Press, New York.

Pankiwskyj, K. A. (1978) *Bedrock Geology of the Dixfield Quadrangle, Maine*, scale 1:62 500. Maine Geological Survey Open-file Map **78-15**.

Pasteels, P. and Doré, F. (1982) Age of the Vire-Carolles granite. In *Numerical Dating and Stratigraphy, Part II*, ed G. S. Odin, pp. 784–790. Wiley, New York.

Peltzer, G., Tapponnier, P. and Cobbold, P. (1982) Les grands décrochements de l'Est Asiatique: évolution dans le temps et comparaison avec un modèle expérimental. *Comptes rendus de l'Academie des Sciences, Paris* **294**, 1341–1348.

Peterson, V. L. and Robinson, P. (1993) Progressive evolution from uplift to orogen-parallel transport in a late-Acadian, upper amphi-

bolite- to granulite-facies shear zone, south-central Massachusetts. *Tectonics* **12**, 550–567.

Peucat, J.-J. (1986) Behavior of Rb–Sr whole-rock and U–Pb zircon systems during partial melting as shown in migmatitic gneisses from the Saint Malo Massif, NE Brittany, France. *Journal of the Geological Society of London* **143**, 875–885.

Román-Berdiel, T., Gapais, D. and Brun, J.-P. (1997) Granite intrusion along strike-slip zones in experiment and nature. *American Journal of Science* **297**, 651–678.

Royden, L. H. (1993) The steady state thermal structure of eroding orogenic belts and accretionary prisms. *Journal of Geophysical Research* **98**, 4487–4507.

Rutter, E. H. (1997) The influence of deformation on the extraction of melts: A consideration of the role of melt-assisted granular flow. In *Deformation-enhanced Melt Segregation and Metamorphic Fluid Transport*, ed. M. Holness. The Mineralogical Society Series. Chapman and Hall, London.

Rutter, E. H. and Brodie, K. H. (1992) Rheology of the lower crust. In *Continental Lower Crust*, eds D. M. Fountain, R. Arculus and R. W. Kay, pp. 201–267. Developments in Geotectonics 2. Elsevier, Amsterdam.

Rutter, E. H. and Brodie, K. H. (1995) Mechanistic interactions between deformation and metamorphism. *Geological Journal* **30**, 227–239.

Rutter, E. H. and Neumann, D. H. K. (1995) Experimental deformation of partially molten Westerly granite under fluid-absent conditions, with implications for the extraction of granitic magma. *Journal of Geophysical Research* **100**, 15697–15715.

Schumacher, J. C., Hollocher, K. T., Robinson, P. and Tracy, R. J. (1990) Progressive reactions and melting in the Acadian metamorphic high of central Massachusetts in southwestern New Hampshire, USA. In *High-temperature Metamorphism and Crustal Anatexis*, eds J. R. Ashworth and M. Brown, pp. 198–234. Unwin Hyman, New York.

Smith, H. A. and Barreiro, B. (1990) Monazite U–Pb dating of staurolite grade metamorphism in pelitic schists. *Contributions to Mineralogy and Petrology* **105**, 602–615.

Solar, G. S. (1996) Relationship between ductile deformation and granitic magma transfer: Tumbledown Mountain area, west-central Maine. In *Guidebook to Fieldtrips in Northern New Hampshire and Adjacent Regions of Maine and Vermont, New England Intercollegiate Geological Conference*, pp. 341–362. 88th Annual Meeting, Trip C5.

Stewart, D. B., Wright, B. E., Unger, J. D., Phillips, J. D. and Hutchinson, D. R. (principal compilers) (1992) *Global Geoscience Transect 8: Quebec–Maine–Gulf of Maine Transect, Southeastern Canada, Northeastern United States of America*. U.S. Department of the Interior, U.S. Geological Survey, to accompany map **I-2329**.

Strachan, R. A., Treloar, P. J., Brown, M. and D'Lemos, R. S. (1989) Cadomian terrane tectonics and magmatism in the Armorican Massif. *Journal of the Geological Society of London* **146**, 423–426.

Thompson, A. B., Schulmann, K. and Jezek, J. (in press) Thermal evolution and exhumation in obliquely convergent (transpressive) orogens. *Tectonophysics*.

Tommasi, A., Vauchez, A. and Daudré, B. (1995) Initiation and propagation of shear zones in a heterogeneous continental lithosphere. *Journal of Geophysical Research* **100**, 22083–22101.

Tommasi, A., Vauchez, A., Fernandes, L. A. D. and Porcher, C. C. (1994) Magma-assisted strain localization in an orogen-parallel transcurrent shear zone of southern Brazil. *Tectonics* **13**, 421–437.

Treloar, P. J. and Strachan, R. A. (1990) Cadomian strike slip tectonics in NE Brittany. In *The Cadomian Orogeny*, eds R. S. D'Lemos, R. A. Strachan and C. G. Topley, pp. 151–168. Geological Society of London Special Publication **51**.

Tullis, J., Yund, R. and Farver, J. (1996) Deformation-enhanced fluid distribution in feldspar aggregates and implications for ductile shear zones. *Geology* **24**, 63–66.

White, S. H. and Knipe, R. J. (1978) Transformation- and reaction-enhanced ductility in rocks. *Journal of the Geological Society of London* **135**, 513–516.

Wolf, M. B. and Wyllie, P. J. (1991) Dehydration-melting of solid amphibolite at 10 kbar: Textural development, liquid interconnectivity and application to segregation of magmas. *Contributions to Mineralogy and Petrology* **44**, 151–179.

Zhang, S., Paterson, M. and Cox, S. F. (1994) The influence of deformation on porosity and permeability in calcite aggregates. *Journal of Geophysical Research* **99**, 15761–15775.